



1-2012

Lymph Node Characterization in Vivo Using Endoscopic Ultrasound Spectrum Analysis With Electronic Array Echo Endoscopes

Ronald Kumon

Aparna Repaka

Case Western Reserve University

Matthew Atkinson

Case Western Reserve University

Ashley L. Faulx

Case Western Reserve University

Richard C.K. Wong

Case Western Reserve University

See next page for additional authors

Follow this and additional works at: https://digitalcommons.kettering.edu/physics_facultypubs

 Part of the [Physics Commons](#)

Recommended Citation

Kumon, Ronald; Repaka, Aparna; Atkinson, Matthew; Faulx, Ashley L.; Wong, Richard C.K.; Isenberg, Gerard A.; Hsiao, Yi-Sing; Gudur, Madhu Sudhan Reddy; Deng, Cheri X.; and Chak, Amitabh, "Lymph Node Characterization in Vivo Using Endoscopic Ultrasound Spectrum Analysis With Electronic Array Echo Endoscopes" (2012). *Physics Publications*. 30.
https://digitalcommons.kettering.edu/physics_facultypubs/30

This Article is brought to you for free and open access by the Physics at Digital Commons @ Kettering University. It has been accepted for inclusion in Physics Publications by an authorized administrator of Digital Commons @ Kettering University. For more information, please contact digitalcommons@kettering.edu.

Authors

Ronald Kumon, Aparna Repaka, Matthew Atkinson, Ashley L. Faulx, Richard C.K. Wong, Gerard A. Isenberg, Yi-Sing Hsiao, Madhu Sudhan Reddy Gudur, Cheri X. Deng, and Amitabh Chak

Lymph node characterization in vivo using endoscopic ultrasound spectrum analysis with electronic array echo endoscopes

Authors

R. E. Kumon^{1,2}, A. Repaka^{3,4}, M. Atkinson³, A. L. Faulx³, R. C. K. Wong³, G. A. Isenberg³, Y.-S. Hsiao¹, M. S. R. Gudur¹, C. X. Deng¹, A. Chak³

Institutions

Institutions are listed at the end of article.

submitted 1. July 2011
accepted after revision
10. January 2012

Bibliography

DOI <http://dx.doi.org/10.1055/s-0032-1306774>
Endoscopy 2012; 44: 618–621
© Georg Thieme Verlag KG
Stuttgart · New York
ISSN 0013-726X

Corresponding author

R. E. Kumon, PhD
Department of Physics
Kettering University
1700 University Ave., Flint
Michigan, 48504-6214
USA
Fax: +1-810-762-7830
research@kumonweb.com

Our purpose was to demonstrate the use of radio-frequency spectral analysis to distinguish between benign and malignant lymph nodes with data obtained using electronic array echo endoscopes, as we have done previously using mechanical echo endoscopes. In a prospective study, images were obtained from eight patients with benign-appearing lymph nodes and 11 with malignant lymph nodes, as verified by fine-needle aspiration. Midband fit, slope, intercept, correlation coefficient, and root-mean-square (RMS) deviation from a linear regression of the calibrated power spectra were determined and compared

between the groups. Significant differences were observable for mean midband fit, intercept, and RMS deviation (t test $P < 0.05$). For benign ($n = 16$) vs. malignant ($n = 12$) lymph nodes, midband fit and RMS deviation provided classification with 89% accuracy and area under receiver operating characteristic (ROC) curve of 0.95 based on linear discriminant analysis. We concluded that the mean spectral parameters of the backscattered signals from electronic array echo endoscopy can provide a noninvasive method to quantitatively discriminate between benign and malignant lymph nodes.

Introduction

Endoscopic ultrasound (EUS) is often employed for locoregional staging of gastrointestinal malignancy. However, differentiating between benign and malignant lymph nodes is still sometimes difficult based on EUS appearance alone [1,2]. Although EUS-guided fine needle aspiration (FNA) can obtain diagnostic cytologic material, targeting of tissue for FNA still depends on imaging, and there is still an important need for better methods for distinguishing benign from neoplastic tissue. Our previous studies with mechanical echo endoscopes have shown that spectral parameters from backscattered signals can be used to quantitatively distinguish between benign and malignant lymph nodes [3,4].

In spectrum analysis, the radiofrequency (RF) data of the ultrasound energy that is backscattered from local tissue inhomogeneities is analyzed [5]. The nature of the backscattered signals depends on the effective size and acoustic concentration of the scattering tissues as well as the local variations in acoustic impedance (product of density and sound speed). Different tissue types may then be distinguished because they have different microstructures that scatter ultrasound differently. Spectral parameters provide a

quantitative assessment that is independent of the system being used and of the user, given proper calibration. In the context of gastrointestinal cancer, ex vivo studies of lymph node metastases of colorectal cancer have shown that ultrasound backscatter analysis performed better than B-mode ultrasound [6] even when multiple B-mode sonographic parameters were considered [7]. Recent investigations using high frequency ultrasound (25.6 MHz center frequency) to examine ex vivo lymph node specimens have shown specificity and sensitivity as high as 95% with multiple backscatter parameters [8,9].

Over the past decade, radial and curvilinear electronic array echo endoscopes have widely replaced mechanical echo endoscopes. Our aim in this study was to test the ability of spectral analysis of EUS backscattered signals to distinguish between benign and malignant lymph nodes using data obtained from electronic array echo endoscopes.

Patients and methods



Diagnostic criteria

Patients in the benign node group met all of the following criteria: (i) referred for EUS for reasons other than cancer staging; (ii) no prior or current diagnosis of malignancy; (iii) no identification of mass lesions at EUS; (iv) each lymph node showing at least one of the following EUS features suggestive of benign nodes: (a) draping configuration (b) hyperechoicity (c) node diameter < 1 cm; (v) no diagnosis of cancer in the year following EUS examination as determined by follow-up telephone questionnaire and/or review of medical records.

Patients in the malignant node group met both the following criteria: (i) lymph node identified at EUS; (ii) FNA cytology positive for carcinoma.

Patients

A total of 19 patients were included in the study. FNA-proven malignant lymphadenopathy was shown in 11 patients, associated with malignancy of the pancreas (n=3), lymphoma (n=2), rectum (n=1), lung (n=2), and esophagus (n=3). Benign-appearing lymph nodes were imaged in eight patients, without a diagnosis of malignancy. Indications for these procedures were incidental mediastinal adenopathy (n=3), benign pancreatic disease (n=4), and gastrointestinal stromal tumor (GIST) (n=1). In some cases, multiple lymph nodes were imaged in a patient.

RF data acquisition and analysis

We used radial (GF-UE160-AL5) and curvilinear (GF-UC140P-AL5) electronic-array ultrasonic gastrovideoscopes operated in the 6MHz mode with a commercially available clinical ultrasound system (Exera EU-ME1; Olympus America, Center Valley, Pennsylvania, USA). The echo endoscopes contain ultrasound transducer arrays which are electronically excited in sets to generate 360° (radial) or 180° (curvilinear) B-scan cross-sectional images, composed of hundreds of A-scan lines. Each image and its corresponding RF data were simultaneously digitized by the Exera EU-ME1 system and automatically saved.

We then imported the RF data into our custom-designed analysis software (written using MATLAB 2010b; Mathworks, Natick, Massachusetts, USA) for offline image reconstruction and data processing. We independently verified that the gain, contrast, line density, and frame correlation settings, which affect the appearance of the system image, did not change the underlying RF data acquired by the system.

Prior to RF data analysis, clinical endoscopists identified and manually segmented regions of interest (ROIs) on the system image according to the evaluation criteria described below. Data analysts then independently translated the ROIs onto the reconstructed image to select corresponding segments of RF data. The sector-shaped ROIs were maximized in size within the designated areas. The fast Fourier transform (FFT) was used to find the power spectra for each segment of A-scan RF data within the ROI after gating the segment by a series of sliding Hamming windows of $0.8\mu\text{s}$ (~0.62 mm), each offset by $0.1\mu\text{s}$ (~0.077 mm).

• **Fig. 1 a** shows a typical example of an ROI chosen for a lymph node using the curvilinear echoendoscope, while • **Fig. 1 b** shows that the FNA used to determine the malignancy of the node was obtained in the same tissue area under EUS guidance.

Spectrum calibration

Previous studies have typically removed the artifacts associated with the composite transfer function of the electronic transmitter/receiver and transducer of the EUS system by dividing the power spectrum from the tissue by the spectrum of an ideal reflector. However, we did not have control over the electronic gain settings for the RF data acquisition (not the image gain setting), and, as such, we could not use a strong ultrasound reflector (e.g., glass) without saturating the received signal from an ideal reflector. Instead, calibration was performed using reflections from the flat wall of an acrylic plastic chamber filled with an attenuating gelatin-based phantom [4]. The phantom material was independently measured using the substitution method to have an attenuation of 1.5 dB/MHz/cm, which was sufficient to prevent signal saturation while minimally affecting overall spectral shape.

To obtain the RF calibration data, an 18-mm hole in the phantom was filled with water. We then inserted the transducer, and inflated the endoscope's balloon with water until the balloon was in full contact with the phantom. We manually adjusted the orientation of the endoscope tip to make the central axis of the endoscope parallel to the wall. We then acquired the RF data, and computed by spectrum by FFT. The calibration spectrum was then compensated for round-trip attenuation. To obtain the calibrated spectra, we then divided the tissue spectra by the calibration spectrum.

Because the calibrated spectra are typically quasilinear over the ultrasound frequency band used [3], they can be effectively characterized by linear regression using their slope, intercept, and their midband fit, which is the value of the linear function eval-

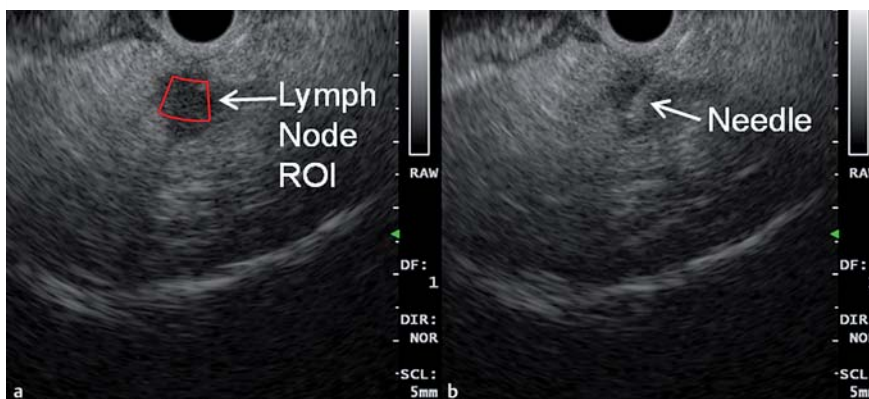


Fig. 1 Lymph node characterization in vivo using endoscopic ultrasound (EUS) and radiofrequency (RF) spectrum analysis: selection of region of interest (ROI), and fine needle aspiration (FNA).

a System image of a lymph node showing superimposed typical ROI selection. The RF EUS data underlying the image was acquired prior to FNA.

b EUS-guided FNA of the same tissue area. Subsequent cytological analysis showed that the node was malignant.

Table 1 Lymph node characterization in vivo using endoscopic ultrasound (EUS) and radiofrequency spectrum analysis. Descriptive statistics and hypothesis testing results for lymph node data. Columns 2 and 3 show the means and standard deviations of spectral parameters averaged over the regions of interest for benign and malignant lymph nodes. Column 4 lists the *P* values resulting from application of Student's *t* test, assuming equal variance between groups.

	Benign lymph nodes (n=16)	Malignant lymph nodes (n=12)	<i>P</i> value
<i>Mean spectral parameter</i>			
Midband fit, dB	-61.3 ± 4.8	-69.0 ± 4.1	<0.001
Slope, dB/MHz	0.087 ± 0.57	0.28 ± 0.79	0.16
Intercept, dB	-60.7 ± 3.7	-70.8 ± 9.2	<0.001
Correlation coefficient <i>R</i> ²	0.29 ± 0.08	0.27 ± 0.08	0.54
RMS deviation, dB	4.32 ± 0.30	5.07 ± 0.49	<0.001

RMS, root-mean-square

Table 2 Lymph node characterization in vivo using endoscopic ultrasound (EUS) and radiofrequency spectrum analysis. Results from linear discriminant analysis of lymph node data. Classification was performed using midband fit and root-mean-square (RMS) deviation as independent variables, and the reported values used "leave-one-out" cross-validation. The overall accuracy of classification was 89%. (See Fig. 2 for the corresponding scatterplot and receiver operating characteristic [ROC] curve.)

Tissue state	Predicted state, n (%)		Total
	Malignant	Benign	
Malignant	10 (83.3)	2 (16.7)	12 (100)
Benign	1 (6.3)	15 (93.8)	16 (100)

uated at the midpoint of the -15-dB frequency bandwidth. We corrected both the midband fit and slope values for the attenuation of the intervening tissue between the transducer and the ROI, using an assumed attenuation of 0.5 dB/MHz/cm; the intercept is not affected by this attenuation correction [5]. We also recorded the square of the correlation coefficient, *R*², and the root-mean-square (RMS) deviation of the regression line as normalized and unnormalized measures of the deviation of the calibrated spectrum from linearity.

Statistical analysis.

To obtain a single value for each ROI, we averaged the spectral parameters generated from each window over each ROI. We then analyzed the resulting values using Student's *t* test for independent samples. The *t* tests assumed equal variance, and all parameters satisfied the Shapiro–Wilk normality test. Once we had identified parameters that had statistically significant differences between group means, we performed linear discriminant analysis (LDA) to classify the data using equal prior probabilities for each group and the within-groups covariance matrix. For LDA where the same data was used for training and testing, we used the leave-one-out approach for cross-validation.

We performed all statistical calculations using SPSS (Version 16, SPSS, Chicago, Illinois, USA). We fitted a binormal receiver operating characteristic (ROC) curve to the resulting discriminant scores by using ROCKIT (Version 1.1B2, University of Chicago, Chicago, IL, USA), and then assessed classification performance by computing the area under the ROC curve (AUC) from ROCKIT.

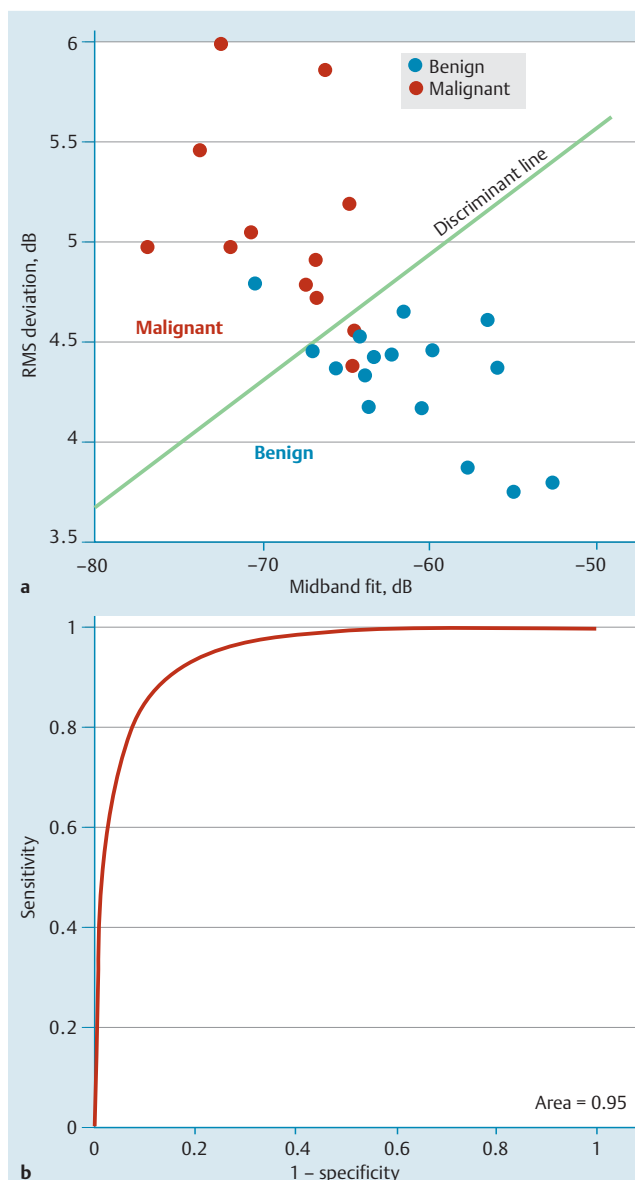


Fig. 2 Linear discriminant analysis (LDA) and receiver operating characteristic (ROC) curve for the lymph node data. **a** Scatterplot of data with coordinates given by midband fit and root mean square (RMS) deviation. The dividing line between benign and malignant classification is based on LDA. **b** Corresponding binormal maximum likelihood estimate of the ROC curve. The area under the curve is 0.95 (See Tab. 2 for the corresponding classification matrix.).

Results



Tab. 1 lists the means and standard deviations of the sets of mean spectral parameters obtained from averaging over the ROIs for each benign and malignant lymph node. The *t* tests showed that midband fit, intercept, and RMS deviation were significantly different between the benign and malignant nodes with the malignant nodes having lower midband fit and intercept, but greater RMS deviation.

Tab. 2 shows the results of the LDA classification using midband fit and RMS deviation and leave-one-out cross-validation. The canonical discriminant function coefficients were -0.108 for the midband fit, and 1.704 for the RMS deviation, with a constant value of -14.877. (The use of intercept and RMS deviation or in-

tercept and midband fit gave comparable or worse results.) With the malignant outcome considered a “positive” test result, the classification had sensitivity of 83%, specificity of 94%, positive predictive value of 91%, negative predictive value of 88%, and overall accuracy of 89%.

• **Fig. 2a** shows the corresponding scatterplot of the data using midband fit and RMS deviation. The discriminant line shows the approximate dividing line between benign and malignant cases according to the LDA. • **Fig. 2b** shows the corresponding binormal estimate of the ROC curve with AUC of 0.95.

Discussion



In our previous studies, midband fit and intercept were found to best distinguish benign and malignant lymph nodes, although only with a maximum sensitivity of 67%, specificity of 82%, overall accuracy of 73%, and ROC AUC of 0.90 with all data from both studies [4], and therefore below the level of the current results. In those studies two different echo endoscopes had to be used to obtain the RF data and FNA biopsies; however in the current study the curvilinear echoendoscope could obtain both at once (see • **Fig. 1**). It is possible that this factor could account for the improved classification. In the current study we also computed the RMS deviation and found that it provided another relatively uncorrelated parameter for discrimination between the benign and malignant nodes.

The lower midband fit and intercept observed here are consistent with our previous studies with the single-element echo endoscopes. The ability of intercept to distinguish between benign and malignant lymph nodes is consistent with previously reported results for ex vivo lymph nodes, using single-element transducers with metastases from colorectal [6] and breast [10] cancers (−15 dB bandwidth of 4.5–11 MHz) as well as cancerous lymph nodes from breast, colon, and gastric cancers at higher frequencies (−6 dB bandwidth of 16.4–33.6 MHz) [8, 9]. These studies reported higher (less negative) intercepts for metastatic nodes and also observed significant differences in slope between benign and malignant nodes. However, it may be difficult to exactly compare these results with the current study given the different transducer types and more highly controlled conditions of the ex vivo studies.

Additional work will be useful to address the limitations of this study. Because histological results were only available for cases with suspected malignancy (malignant lymph nodes), the benign cases had to be inferred from other more indirect clinical and “classic” EUS diagnosis criteria. As such, the study only included fairly well-defined cases, and additional work is needed to assess the utility of the approach in more ambiguous situations. Also, the modest sample size precluded the use of additional criteria (e.g., texture or morphological parameters) with more sophisticated classification methods (e.g., support vector machines) that could result in an improved ability to discriminate between tissue states.

Conclusion



This study shows that spectral analysis of the EUS RF backscatter signals from radial and curvilinear electronic-array echo endoscopes can discriminate between benign and malignant lymph nodes in vivo. With further development, this method may prove useful for providing real-time “digitally stained” images with coloration corresponding to the probability of various normal or disease states, thereby providing endoscopists with more timely and improved accuracy of diagnosis with EUS.

Competing interests: None

Institutions

¹ Department of Biomedical Engineering, University of Michigan, Ann Arbor, Michigan, USA

² Department of Physics, Kettering University, Flint, Michigan, USA

³ Division of Gastroenterology, University Hospitals Case Medical Center and Case Western Reserve University, Cleveland, Ohio, USA

⁴ University of Medicine and Dentistry of New Jersey, New Brunswick, New Jersey, USA

Acknowledgments



The authors would like to acknowledge Olympus for making the RF data available and for providing technical information about the EU-ME1 system.

This work was supported by University Hospitals Case Medical Center and the University of Michigan. Amitabh Chak was supported by a K24 Midcareer Award in Patient Oriented Research, National Institutes of Health (Grant DK002800).

References

- 1 *Catalano MF, Alcocer E, Chak A et al.* Evaluation of metastatic celiac axis lymph nodes in patients with esophageal carcinoma: accuracy of EUS. *Gastrointest Endosc* 1999; 50: 352–356
- 2 *Bhutani MS, Hawes RH, Hoffman BJ.* A comparison of the accuracy of echo features during endoscopic ultrasound (EUS) and EUS-guided fine-needle aspiration for diagnosis of malignant lymph node invasion. *Gastrointest Endosc* 1997; 45: 474–479
- 3 *Kumon RE, Olowe K, Faulx AL et al.* EUS spectrum analysis for in vivo characterization of pancreatic and lymph node tissue: a pilot study. *Gastrointest Endosc* 2007; 66: 1096–1106
- 4 *Kumon RE, Pollack MJ, Faulx AL et al.* In vivo characterization of pancreatic and lymph node tissue by using EUS spectrum analysis: a validation study. *Gastrointest Endosc* 2010; 71: 53–63
- 5 *Lizzi FL, Feleppa EJ, Alam SK et al.* Ultrasonic spectrum analysis for tissue evaluation. *Pattern Recog Lett* 2003; 24: 637–658
- 6 *Noritomi T, Machi J, Feleppa EJ et al.* In vitro investigation of lymph node metastasis of colorectal cancer using ultrasonic spectral parameters. *Ultrasound Med Biol* 1998; 24: 235–243
- 7 *Tateishi T, Machi J, Feleppa EJ et al.* In vitro investigation of detectability of colorectal lymph nodes and diagnosis of lymph node metastasis in colorectal cancer using B-mode sonography. *J Clin Ultrasound* 2004; 32: 1–7
- 8 *Mamou J, Coron A, Hata M et al.* Three-dimensional high-frequency characterization of cancerous lymph nodes. *Ultrasound Med Biol* 2010; 36: 361–375
- 9 *Mamou J, Coron A, Oelze ML et al.* Three-dimensional high-frequency backscatter and envelope quantification of cancerous human lymph nodes. *Ultrasound Med Biol* 2011; 37: 345–357
- 10 *Tateishi T, Machi J, Feleppa EJ et al.* In vitro diagnosis of axillary lymph node metastases in breast cancer by spectrum analysis of radio frequency echo signals. *Ultrasound Med Biol* 1998; 24: 1151–1159